0026-895X/03/6403-650–658$7.00
MOLECULAR PHARMACOLOGY
Copyright © 2003 The American Society for Pharmacology and Experimental Therapeutics
Mol Pharmacol 64:650–658, 2003

Vol. 64, No. 3
2559/1091341
Printed in U.S.A.

Agonist-Induced Conformational Changes in the Extracellular Domain of α7 Nicotinic Acetylcholine Receptors

LISA K. LYFORD, ADRIAN D. SPROUL, DONNIE EDDINS, JAMES T. MCLAUGHLIN, and ROBERT L. ROSENBERG

Departments of Pharmacology (L.K.L., A.D.S., D.E., J.T.M., R.L.R.) and Cell and Molecular Physiology (R.L.R.), University of North Carolina at Chapel Hill, Chapel Hill, North Carolina

Received April 2, 2003; accepted June 17, 2003

This article is available online at http://molpharm.aspetjournals.org

ABSTRACT

The molecular mechanisms that couple agonist binding to the gating of Cys-loop ionotropic receptors are not well understood. The crystal structure of the acetylcholine (ACh) binding protein has provided insights into the structure of the extracellular domain of nicotinic receptors and a framework for testing mechanisms of activation. Key ligand binding residues are located at the C-terminal end of the β9 strand. At the N-terminal end of this strand (loop 9) is a conserved glutamate [E^{172} in chick α7 nicotinic acetylcholine receptors (nAChRs)] that is important for modulating activation. We hypothesize that agonist binding induces the movement of loop 9. To test this, we used the substituted-cysteine accessibility method to examine agonist-dependent changes in the modification of cysteines introduced in loop 9 of $L^{247}T$ α7 nAChRs. In the absence of agonist, ACh-evoked responses of $E^{172}C/L^{247}T$ α7 nAChRs were inhibited by 2-trimethylammonioethylmethane thiosulfonate (MTSET). Agonist coapplication with MTSET reduced the extent and rate of modification. The dose-dependence of ACh activation was nearly identical with that of ACh-dependent protection from modification. ACh increased the inhibition by methanethiosulfonate reagents of $N^{170}C$ and did not change inhibition of $G^{171}C$ receptors. The antagonist dihydro-β-erythroidine did not mimic the effects of ACh. Combined with a structural model, the data suggest that receptor activation includes subunit rotation and/or intrasubunit conformational changes that move N^{170} to a more accessible position and E^{172} to a more protected position away from the vestibule. Thus, loop 9, located near the junction between the extracellular and transmembrane domains, participates in conformational changes triggered by ligand binding.

Ligand-gated ion channels in the Cys-loop superfamily (ionotropic receptors for glycine, GABA, serotonin, ACh, and others) (Karlin, 2002) mediate fast neurotransmission throughout the nervous system (Hille, 2001). In particular, nicotinic ACh receptors are responsible for excitatory signals at the neuromuscular junction, autonomic ganglia, and a few synapses in the central nervous system (Jones et al., 1999). In addition, presynaptic nicotinic receptors, especially the α7 subtype, modulate the release of neurotransmitters at both excitatory and inhibitory central synapses (Role and Berg, 1996).

Ligand-gated ion channels containing the conserved Cys loop are formed as a rosette of five homologous or identical subunits around a central pore (Karlin, 2002). In each subunit, the N-terminal ~210 residues make an extracellular domain that forms the ligand binding region and the outer vestibule of the ion-conducting pore. The extracellular domain of each subunit is connected to a transmembrane domain consisting of four α helices. The transmembrane pore is lined by the second (M2) helix. The "gate" of the channel, the region that controls whether the channel is in a conducting or nonconducting state, is located at the cytoplasmic end of the M2 helix (Karlin, 2002).

The molecular mechanisms that couple agonist binding in the extracellular domain to the opening of the gate are not well understood. A wave of conformational change is believed to propagate from the ligand binding site to the gate (Grosman et al., 2000). These conformational changes could include symmetric (Unwin et al., 2002) or asymmetric (Horenstein et al., 2001) rotation of the M2 helices, perhaps driven by interactions between the extracellular ligand binding domain and the extracellular loop between the M2 and M3 transmembrane helices (Grosman et al., 2000; Kash et al., 2003).

Our understanding of ligand binding has been advanced greatly by the crystal structure of the ACh binding protein (AChBP) (Brejc et al., 2001). This soluble protein shares sequence homology with the N-terminal ecto-domain of nic-

This work was supported by National Institutes of Health grant NS37317.

ABBREVIATIONS: ACh, acetylcholine; nAChR, nicotinic acetylcholine receptor; DHβE, dihydro-β-erythroidine; MTSET, 2-trimethylammonioethylmethane thiosulfonate; MTSES, 2-sulfonatoethylmethane thiosulfonate; MTS, methanethiosulfonate; AChBP, acetylcholine binding protein; ES-Ca^{2+}, extracellular solution containing Ca^{2+}; ES-EGTA, extracellular solution containing EGTA; BAPTA, 1,2,-bis-(2-aminophenoxy)ethane-*N,N,N′,N′*-tetraacetic acid.

otinic receptor subunits (24% sequence identity with the α7 subunit), contains the archetypal Cys loop, and forms a pentamer around a central cavity. These properties, together with functional ligand binding properties, make the AChBP the best model to date for the structure that forms the extracellular ligand binding domain of Cys-loop ionotropic receptors. Structural details from the AChBP also provide insight into possible mechanisms for the conformational changes associated with gating (Kash et al., 2003).

The structure of the AChBP contains a core of 10 β strands and shows the ligand binding site at the cleft between subunits (Brejc et al., 2001). Among the residues that form the binding site are conserved tyrosines (Y^{187} and Y^{194} in chick α7 numbering) and a vicinal disulfide (C^{189}–C^{190}) that define a region identified previously as essential for ligand binding (Brejc et al., 2001; Karlin, 2002). This region is located at the C terminus of the β9 strand. At the other end of the β9 strand, in loop 9, is a glutamate residue (E^{172} in chick α7) that is conserved among nAChR receptor subunits (except β1) (Elgoyhen et al., 1994, 2001; Le Novere and Changeux, 1995). This glutamate is important for modulating the gating of α7 nAChRs by extracellular Ca^{2+}. In chimeric receptors formed from the N terminus of α7 nAChRs and the transmembrane domain of 5-hydroxytryptamine-3 receptors, the mutation of E^{172} abolishes the enhancement of receptor activation by extracellular Ca^{2+} (Galzi et al., 1996). In nondesensitizing $L^{247}T$ α7 receptors (L9′T in the M2 numbering system) (Revah et al., 1991), mutation of E^{172} to Gln or Cys eliminates the enhancing effects of extracellular Ca^{2+} and other permeant divalent cations (Eddins et al., 2002a,b). Thus, E^{172} is part of a region that mediates a modulatory role of permeant divalent cations on α7 receptor activation.

Because ligand binding involves residues at the C terminus of the β9 strand and Ca^{2+}-dependent modulation is mediated by E^{172} at the N terminus of β9, we reasoned that the transmission of information from the ligand binding site to the gate might involve the β9 strand and its N-terminal loop (loop 9). We tested this hypothesis using the substituted cysteine accessibility method (Karlin and Akabas, 1998) on residues in this loop. We found evidence for agonist-dependent movement of loop 9. Using a model of the α7 extracellular domain derived from the crystal structure of the AChBP, we propose three possible mechanisms that account for the observations. These mechanisms involve the rotation of subunits and/or intrasubunit movement of the β9–β10 hairpin and loop 9.

Materials and Methods

Reagents. Dihydro-β-erythroidine was obtained from Sigma/RBI (Natick, MA). Methanethiosulfonate (MTS) reagents were obtained from Toronto Research Chemicals (Toronto, Canada). Gentamicin was from Invitrogen (Carlsbad, CA). All other reagents were obtained from Fluka (Buchs, Switzerland) or Sigma (St. Louis, MO).

Site-Directed Mutagenesis. $L^{247}T$ (L9′T) α7 receptors were used as the "parent" receptor in this study because of their large current amplitudes and nondesensitizing kinetics (Revah et al., 1991). The mutagenesis of $E^{172}C$ in $L^{247}T$ α7 nAChR cDNA was described previously (Eddins et al., 2002b). Cysteines at other positions were introduced into chick α7 $L^{247}T$ cDNA by site-directed mutagenesis using the QuikChange method (Stratagene, La Jolla, CA). All mutations were confirmed by DNA sequencing.

***Xenopus laevis* Oocyte Maintenance and Expression.** Oocytes were surgically removed from female *X. laevis* frogs in accordance with University of North Carolina Institutional Animal Care and Use Committee guidelines. Oocytes were treated with collagenase to remove follicular cells and were maintained using standard procedures as described previously (Eddins et al., 2002a). cRNA was prepared using the T7 RNA polymerase and mMessage mMachine kit (Ambion, Austin, TX) as described by the manufacturer. Oocytes were injected with 20 ng of cRNA and incubated at 18°C in ND96 (96 mM NaCl, 2 mM KCl, 1.8 mM $CaCl_2$, 1 mM $MgCl_2$, and 5 mM HEPES, pH 7.4) for 2 to 5 days before use.

Two-Electrode Voltage Clamp. Oocytes were superfused in normal extracellular solution containing Ca^{2+} (ES-Ca^{2+}) (96 mM NaCl, 2 mM KCl, 1 mM $MgCl_2$, 2.5 mM $CaCl_2$, and 10 mM HEPES, pH 7.5). In some experiments where indicated, oocytes were bathed in normal extracellular solution containing EGTA (ES-EGTA), in which 2.5 mM $CaCl_2$ was replaced with 1 mM EGTA. Two-electrode voltage clamp was performed with a GeneClamp 500B controlled by pCLAMP6 software (Axon Instruments, Inc., Union City, CA). Electrodes were filled with 3 M KCl contacting Ag-AgCl wires and had resistances of 0.5 to 2.0 MΩ. Currents were recorded at a constant holding potential of −60 mV. Currents were filtered at 50 or 125 Hz and sampled at 250 Hz. To prevent the activation of Ca^{2+}-activated chloride channels, oocytes were injected with 46 nl of 50 mM BAPTA 15 to 60 min before recording (Lyford et al., 2002).

Dose-Response Curves. Agonist dose-response curves were obtained as described previously (Eddins et al., 2002a), and data were fit to the Hill equation using Prism software (GraphPad Software Inc., San Diego, CA). Inhibitory dose-response curves were obtained in the presence of approximate EC_{50} concentrations of ACh.

Modification by MTS Reagents. MTS reagents (Karlin and Akabas, 1998) were prepared daily in water and stored on ice. Because these reagents have a short half-life in physiological buffer, they were diluted to the appropriate working concentration in recording buffer immediately before applying to the oocytes. MTS reagents were applied by continuous flow for 60 s in the presence or absence of agonists or antagonists followed by a 5-min wash in extracellular solution. For each mutant, we tested high concentrations of MTS reagents (~1 mM) to determine the maximal effect of modification. Limiting doses were then used to evaluate differences in the modification between liganded and unliganded receptors. For coapplication experiments, we used a maximal dose of agonist or antagonist (~10 × EC_{50}). Currents evoked by ~75% of the maximal ACh doses (~3 × EC_{50}) were compared before and after MTS treatment to assess the effects of modification. For coapplications, data were normalized to the percentage inhibition (if any) of 60-s applications of the agonist or antagonist alone. At least two oocyte batches from different frogs were tested for each experimental treatment.

Rates of Modification by MTSET. Before assessing rates of reaction, a maximal dose of ACh was applied every 3 min until consistent responses were achieved. MTSET with or without ACh (maximal dose) was repeatedly applied by continuous flow. Between treatments, oocytes were washed with ES-Ca^{2+} for 5 min, and responses to ACh were measured. Data were fit to the equation $I_t = I_{\text{infinity}} + (I_o - I_{\text{infinity}})e^{(-kt)}$, where I_t is the current at time t, I_{infinity} is the current after complete modification (1 mM MTSET), I_o is the initial current before MTSET modification, k is the pseudo first-order rate constant, and t is cumulative time of exposure to MTSET. The pseudo first-order rate constants were converted into second-order rate constants ($M^{-1}s^{-1}$) by dividing by the concentration of MTSET.

Homology Model of the Extracellular Domain of α7 Receptors Based on AChBP. A model of the chick α7 nicotinic receptor was constructed from the coordinates of the ACh binding protein (Brejc et al., 2001), as described previously (Eddins et al., 2002b).

Results

Most Receptors with Cys Substitutions at the N Terminus of the β9 Strand Are Functional. Table 1 shows the ACh EC_{50} values, maximal current amplitudes, and Hill coefficients for the receptors bearing the Cys substitutions used in this study. All receptors were functional except for $W^{173}C/L^{247}T$ α7 receptors. Tryptophan-173 is conserved among nicotinic receptor subunits (Le Novere and Changeux, 1995) and thus may be essential for proper folding, gating, and/or ligand binding. Cys substitutions at other positions were tolerated, although the EC_{50} values of the mutant receptors were higher than that of the parent $L^{247}T$ α7 receptors. In particular, receptors bearing the $E^{172}C$ mutation had an EC_{50} that was ~100-fold greater than the parent receptors. Previous studies (Eddins et al., 2002b) have shown this site to be important for the modulation of activation, so the observed difference in EC_{50} is not surprising. Cys mutants with similar differences in EC_{50} from wild-type receptors have also been used to characterize functional motifs of muscle nAChRs, $GABA_A$ receptors, and 5-hydroxytryptamine-3 receptors (Akabas et al., 1992; McLaughlin et al., 1995; Bera et al., 2002; Panicker et al., 2002).

ACh Reduces the Extent of Modification of $E^{172}C$ by MTSET. Figure 1A shows traces of ACh-evoked currents from $E^{172}C/L^{247}T$ α7 nAChRs before and after MTSET treatment. MTSET inhibited 94% of the ACh-evoked current. After coapplication of 10 μM MTSET with a maximal dose of ACh, however, the ACh-evoked currents were inhibited by only 45% (Fig. 1B). A subsequent application of 10 μM MTSET inhibited 94% of the remaining current, indicating that some cysteines were unmodified during the coapplication of ACh and MTSET. MTSET had no effect on ACh-evoked currents of $E^{172}Q/L^{247}T$ receptors (Fig. 1C) or $L^{247}T$ α7 receptors (Eddins et al., 2002b), indicating specific reaction with Cys-172. These results suggest that agonist-dependent reduction in the effects of MTSET were caused by changes in the extent of modification of $E^{172}C$.

Several mechanisms could explain the reduced inhibition by MTSET during ACh coapplication. ACh could have directly shielded $E^{172}C$ from reaction with MTSET by steric occlusion. However, ACh at the ligand binding site is unlikely to directly occlude MTSET access to $E^{172}C$, because this residue is located at a vestibule-lining position, and the ligand binding site is on the outer surface, ~25 Å away. On the other hand, ACh could directly protect $E^{172}C$ from MTSET during open-channel block (Sine and Steinbach, 1984). This block, however, occurs only at high concentrations of ACh (>300 μM). In addition, the voltage-dependence of block sug-

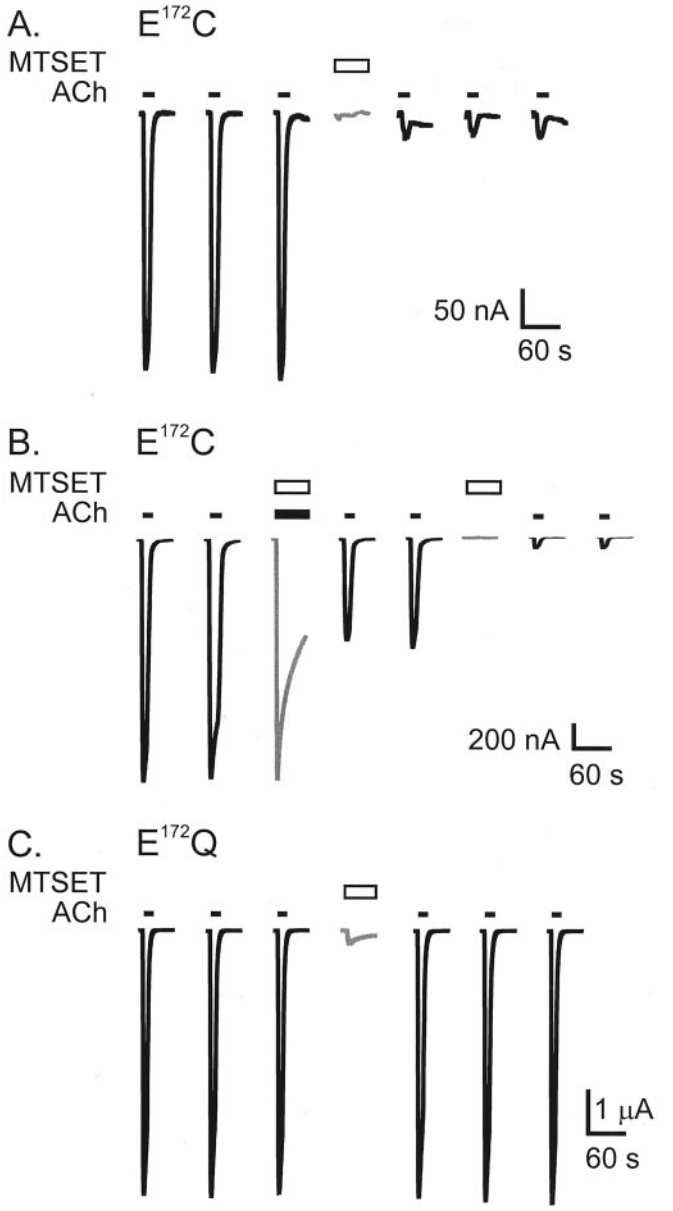

Fig. 1. ACh coapplication reduces the inhibition of $E^{172}C/L^{247}T$ α7 nAChRs by MTSET. Currents were evoked by 10- to 20-s applications of 100 μM ACh (▪) before and after MTSET treatment. A, $E^{172}C/L^{247}T$ α7 nAChRs were inhibited 94 ± 1% (n = 8) after application of 10 μM MTSET (□). B, $E^{172}C/L^{247}T$ α7 nAChRs were inhibited 45 ± 4% (n = 4) after coapplication of 10 μM MTSET (□) and 300 μM ACh (■). Subsequent application of 10 μM MTSET on the same cells resulted in 94 ± 1% (n = 4) inhibition of subsequent ACh-evoked currents. C, control $E^{172}Q/L^{247}T$ α7 nAChRs were unaffected by the application of 1 mM MTSET (n = 5).

TABLE 1

Properties of $L^{247}T$ α 7 nAChR cysteine mutants

Maximum currents were evoked by ACh at ~10 × EC_{50} doses in ES-Ca^{2+} at ≥3 days of expression, except for $L^{247}T$ (≥2 days of expression). Data are presented as mean ± S.E.M.

α7 nAChR Mutant	ACh EC_{50}	n_H	n, No. of Batches	I_{max} (n, No. of batches)
	μM			nA
$L^{247}T$	0.34 ± 0.03[a]	2.3 ± 0.6	6,2	2834 ± 610 (20,7)
$N^{170}C/L^{247}T$	1.9 ± 0.3	1.3 ± 0.2	3,1	170 ± 41 (21,7)
$G^{171}C/L^{247}T$	1.8 ± 0.2	1.4 ± 0.2	5,2	978 ± 214 (8,2)
$E^{172}C/L^{247}T$	38 ± 3	1.9 ± 0.2	8,3	750 ± 205 (25,11)
$D^{174}C/L^{247}T$	3.7 ± 0.2	2.2 ± 0.3	3,1	73 ± 25 (5,2)

[a] Data from Eddins et al. (2002a).

gests that ACh must enter into the transmembrane electric field, which is unlikely to extend to the extracellular vestibule. Thus, this type of direct steric occlusion of MTSET is also unlikely. An alternative to steric occlusion is the possibility that receptor activation causes a conformational change at or around $E^{172}C$, moving it to a position that is less reactive or less accessible to MTSET. Similarly, the movement of residues surrounding $E^{172}C$ (rather than of $E^{172}C$ itself) could have hindered MTSET access or reaction to the substituted Cys. The presence of ACh could also have caused a change in charge distribution near the reaction site, slowing the diffusion of MTSET to the Cys residue, and thus slowing the reaction rate (Karlin and Akabas, 1998). These possibilities are explored below.

Dose-Responses of ACh-Dependent Protection from MTSET Modification and ACh-Dependent Activation Are Similar. To test the hypothesis that the reduced modification of $E^{172}C$ correlates with receptor activation, MTSET was coapplied with varying doses of ACh. Figure 2 displays the fraction of ACh-evoked current remaining after MTSET modification as a function of the coapplied concentrations of ACh (shaded bars, left axis). In comparison, the dose-response curve for ACh-evoked currents had a similar dose-dependence profile (Fig. 2, circles and line fit, right axis). Thus, there was a good correlation between the amount of receptor activation by ACh and the amount of ACh-dependent protection from MTSET modification. These data support the interpretation that ACh-dependent protection from MTSET modification is caused by receptor activation and not by direct steric occlusion.

Epibatidine also Inhibits the Modification of $E^{172}C$ by MTSET. To further test the hypothesis that activation induces a conformational change that inhibits the modification of $E^{172}C$ by MTSET, we tested epibatidine, a nicotinic agonist that is structurally dissimilar to ACh (Gerzanich et

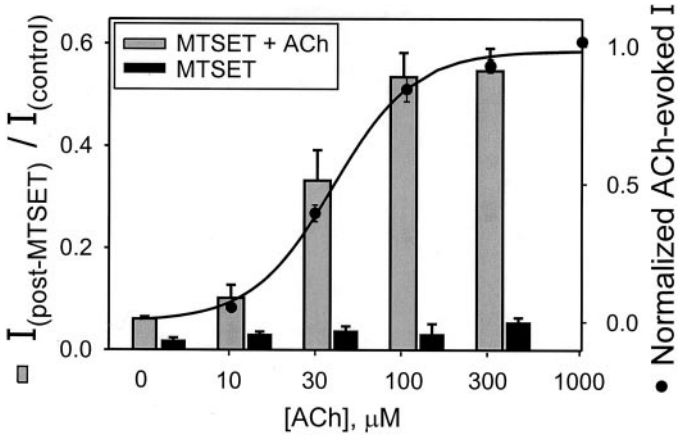

Fig. 2. The dose-dependence of ACh inhibition of MTSET modification correlates with the dose-dependence of ACh activation. ▨, fraction of ACh-evoked current remaining after the coapplication of 10 μM MTSET plus ACh at the concentrations indicated ($n = 4$). Data were normalized to the fractional current remaining after a 60-s application of that concentration of ACh alone. The EC_{50} of ACh inhibition of MTSET modification was 27 ± 6 μM. ■, current remaining after treatment with 10 μM MTSET alone after MTSET plus ACh coapplication ($n = 4$). ●, normalized ACh dose-response of $E^{172}C/L^{247}T$ α7 receptors. The solid line is a fit of the dose-response data to the Hill equation, with an EC_{50} of 38 ± 3 μM and a Hill coefficient of 1.8 ± 0.2 ($n = 8$).

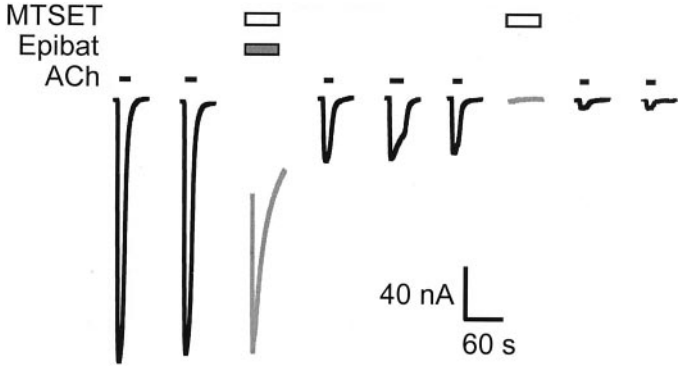

Fig. 3. The agonist epibatidine also reduces the inhibition by MTSET at $E^{172}C$. Coapplication of 3 μM epibatidine (▨) and 10 μM MTSET (□) inhibited 61 ± 3% of subsequent 100 μM ACh-evoked currents ($n = 4$). Application of 10 μM MTSET alone (□) inhibited 92 ± 1% ($n = 3$) of the remaining ACh-evoked currents. Epibatidine activated these receptors with an EC_{50} of 0.31 ± 0.03 μM ($n = 3$).

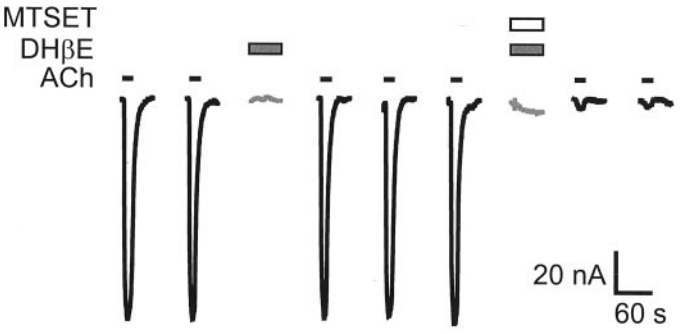

Fig. 4. Coapplication of antagonist DHβE did not decrease MTSET inhibition at $E^{172}C$. Application of 100 μM DHβE alone (▨) had no effect on subsequent ACh-evoked currents ($n = 4$). Coapplication of 10 μM MTSET (□) plus 100 μM DHβE resulted in 99 ± 1% inhibition ($n = 4$), similar to that observed with MTSET alone (see Fig. 1A). DHβE was an antagonist of $E^{172}C/L^{247}T$ α7 nAChRs with an IC_{50} of 15 ± 6 μM (in the presence of 100 μM ACh; $n = 3$, data not shown).

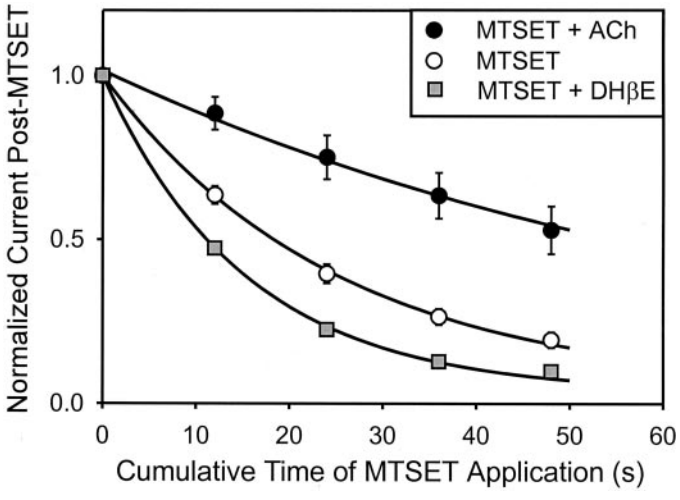

Fig. 5. Rates of $E^{172}C$ modification by MTSET are slower in the presence of ACh and faster in the presence of DHβE. Data are plotted as the normalized ACh-evoked current after treatment with 10 μM MTSET ± 100 μM ACh versus the cumulative time of MTSET exposure. In the absence of ACh, the rate constant was 4,000 ± 200 $M^{-1}s^{-1}$ (○, $n = 9$ from three batches). In the presence of 100 μM ACh, the rate of reaction decreased to 1,400 ± 200 $M^{-1}s^{-1}$ (●, $n = 6$ from three batches). In the presence of 100 μM DHβE, the rate of reaction increased to 6,600 ± 200 $M^{-1}s^{-1}$ (▨, $n = 6$ from two batches). Where not visible, error bars are smaller than the symbols. Rates of reaction were significantly different ($p < 0.001$).

al., 1995). Epibatidine was a full agonist of $E^{172}C/L^{247}T$ $\alpha7$ receptors with an EC_{50} of 0.31 μM (data not shown). Coapplication of 10 μM MTSET with 3 μM epibatidine inhibited 61% of the subsequent ACh-evoked current (Fig. 3). Subsequent treatment with 10 μM MTSET alone inhibited most of the remaining current (Fig. 3). Thus, epibatidine, like ACh, reduced the extent of MTSET modification. These results with differently structured agonists are also consistent with the hypothesis that activation decreases the accessibility or reactivity of $E^{172}C$ caused by a conformational change.

The Antagonist DHβE Does Not Inhibit the Modification of $E^{172}C$. If the modification of $E^{172}C$ by MTSET is decreased by an agonist-induced conformational change rather than by simple occupancy of the binding site, then a similar decrease should not be observed in the presence of a competitive antagonist. We confirmed that DHβE was an antagonist of $E^{172}C/L^{247}T$ $\alpha7$ receptors with an IC_{50} of 15 μM (data not shown). As has been shown for other E^{172} mutations (Eddins et al., 2002b), DHβE showed no agonist activity on $E^{172}C/L^{247}T$ $\alpha7$ receptors and had no effect on subsequent ACh-evoked currents (Fig. 4). When MTSET was coapplied with 100 μM DHβE, subsequent ACh-evoked currents were almost completely inhibited (99%) (Fig. 4). This inhibition was similar to the amount of inhibition obtained by MTSET alone (Fig. 1). Thus, the agonist-dependent inhibition of $E^{172}C$ modification by MTSET required activation of the receptor, not just occupancy of the ligand binding site.

Rates of MTSET Modification Are Decreased in the Presence of ACh and Increased by DHβE. ACh-dependent inhibition of $E^{172}C$ modification should be reflected as an ACh-dependent decrease in the rate of reaction (Karlin and Akabas, 1998). Figure 5 shows that this difference in reaction rates was observed. The rate of MTSET modification of $E^{172}C$ decreased from 4,000 $M^{-1}s^{-1}$ in the absence of ACh to 1,400 $M^{-1}s^{-1}$ in the presence of 100 μM ACh. In contrast, the rate of modification was increased to 6,600 $M^{-1}s^{-1}$ in the presence of 100 μM DHβE, suggesting that the antagonist

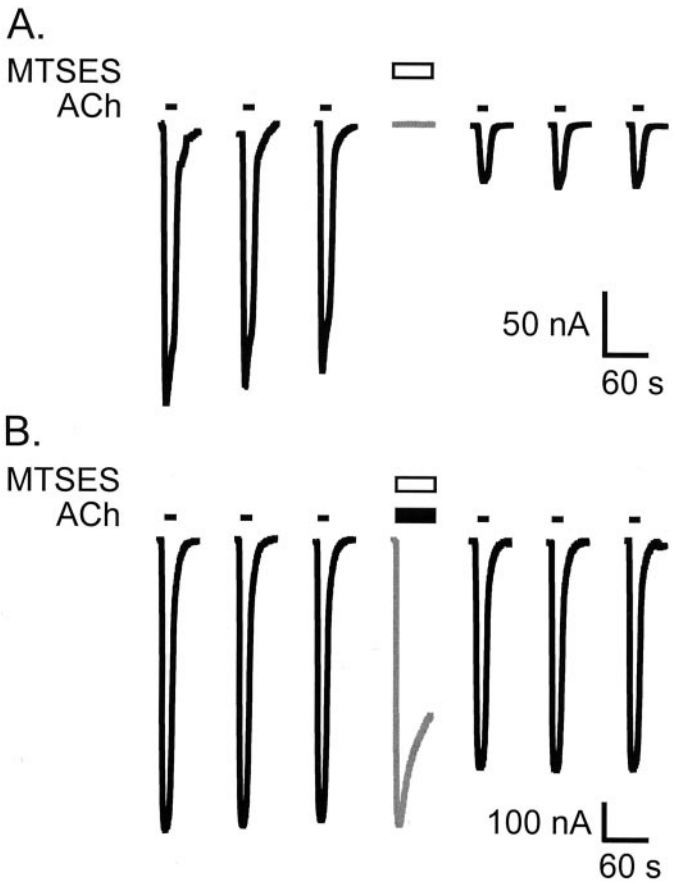

Fig. 6. ACh attenuates the modification at $E^{172}C$ by MTSES. A, treatment with 300 μM MTSES (□) inhibited 73 ± 1% (n = 5) of ACh-evoked currents. B, coapplication of 300 μM MTSES and 300 μM ACh (■) inhibited 11 ± 3% (n = 6) of ACh-evoked currents. Subsequent treatment with MTSES alone (300 μM) inhibited 74 ± 5% (n = 5) of remaining currents (data not shown).

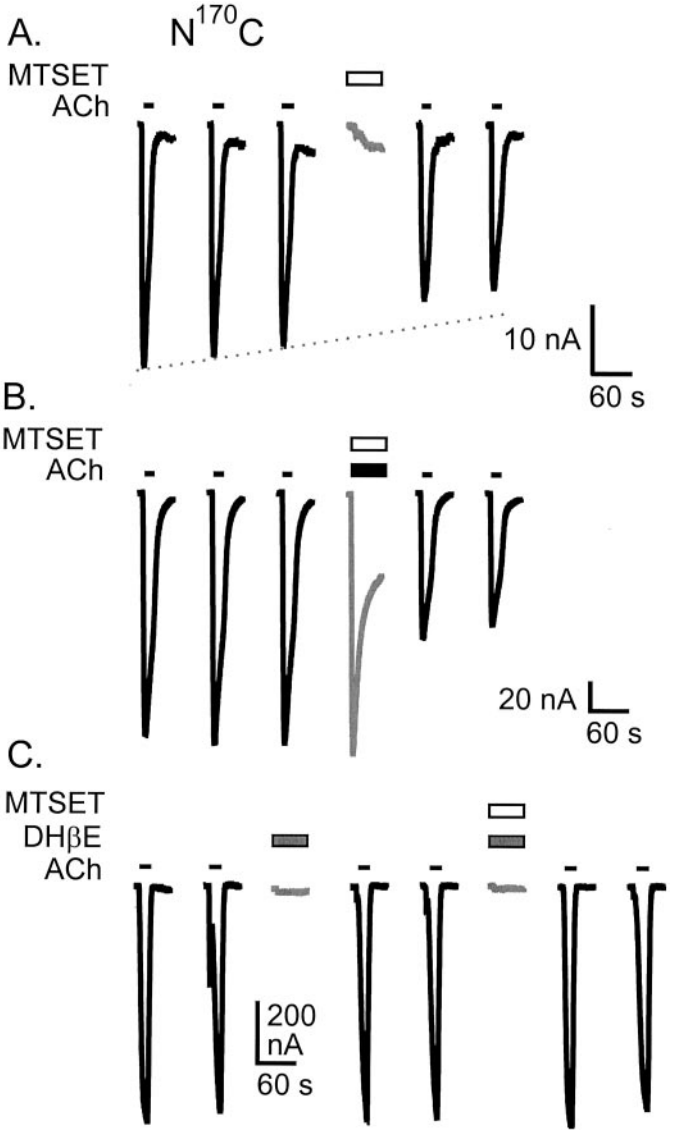

Fig. 7. ACh increases the modification of $N^{170}C$ by MTSET. A, 1 μM MTSET (□) inhibited 14 ± 3% (n = 13) of ACh-evoked currents in ES-Ca^{2+}. The dotted line indicates the rundown adjustment. ▬, 10 μM ACh. B, 1 μM MTSET plus 30 μM ACh (■) inhibited 30 ± 4% (n = 9) of ACh-evoked currents. Similar effects of ACh were observed with MTSET in ES-EGTA and with MTSES (data not shown). MTSET modification rate constants (in ES-Ca^{2+}) were approximately 8,000 ± 2,000 $M^{-1}s^{-1}$ (no ACh; n = 4) and 16,000 ± 3,000 $M^{-1}s^{-1}$ (30 μM ACh, n = 5). C, application of 100 μM DHβE (▨) in ES-EGTA had no effect on subsequent ACh-evoked currents (n = 4). Coapplication of 1 μM MTSET plus 100 μM DHβE had a minimal effect on ACh-evoked currents (n = 7). DHβE was an antagonist of $N^{170}C/L^{247}T$ $\alpha7$ nAChRs with an IC_{50} of 2.6 ± 0.2 μM (in ES-EGTA with 10 μM ACh; n = 3, data not shown).

caused conformational changes that were different from those driven by agonists. The rates of $E^{172}C$ modification are in the same order of magnitude as the rates of modification of accessible residues in the M2 domain (Wilson and Karlin, 2001). The difference in rates with and without ACh was smaller than agonist-dependent differences observed in the M2 domain (Karlin and Akabas, 1995), but it was similar to those observed during allosteric interactions between GABA, benzodiazepine, and pentobarbital binding sites of $GABA_A$ receptors (Teissere and Czajkowski, 2001; Holden and Czajkowski, 2002). The modest difference in rates we observed is expected if the N terminus of β9 is important for conformational changes caused by gating but is not the gate itself.

Modification by MTSES also Inhibits $E^{172}C/L^{247}T$ Receptors and Is Reduced in the Presence of ACh. To determine whether ACh reduced the reactivity of $E^{172}C$ to MTSET by an electrostatic mechanism, we tested the negatively charged MTSES (Karlin and Akabas, 1998). The lowest effective dose of MTSES on $E^{172}C/L^{247}T$ receptors was 300 μM, ~30 times higher than that of MTSET, consistent with the 10-fold slower rates for reactions with MTSES (Karlin and Akabas, 1998). Treatment with MTSES alone inhibited 73% of ACh-evoked currents (Fig. 6A). The inhibition by MTSES indicates that the steric bulk of the MTS adducts, rather than their electrostatic charge, mediates the inhibitory effects of $E^{172}C$ modification. Coapplication with ACh significantly reduced the inhibition by MTSES (Fig. 6B). This suggests that ACh does not alter the modification of $E^{172}C$ by changing the electrostatic environment of the cysteine (Karlin and Akabas, 1998). In addition, these results suggest that the mechanism by which MTS modification of $E^{172}C$ causes a reduction of current amplitudes is not via electrostatic repulsion of permeating ions.

Neighboring Residues. The data so far are consistent with the idea that agonists decrease the accessibility of $E^{172}C$ by causing an activation-dependent conformational change of loop 9 at the N terminus of the β9 strand. If this is the case, activation may also change the accessibility of residues near E^{172}. Thus, we tested the ligand-dependent changes in reactivity of cysteine substitutions of N^{170}, G^{171}, and D^{174} in the $L^{247}T$ α7 receptor background.

ACh Enhances MTSET Inhibition of $N^{170}C/L^{247}T$ α7 Receptors, but DHβE Does Not. $N^{170}C/L^{247}T$ α7 receptors were modestly inhibited (14%) by 1 μM MTSET in the absence of agonist (Fig. 7A), indicating that $N^{170}C$ was at least partially accessible. In the presence of 30 μM ACh, the inhi-

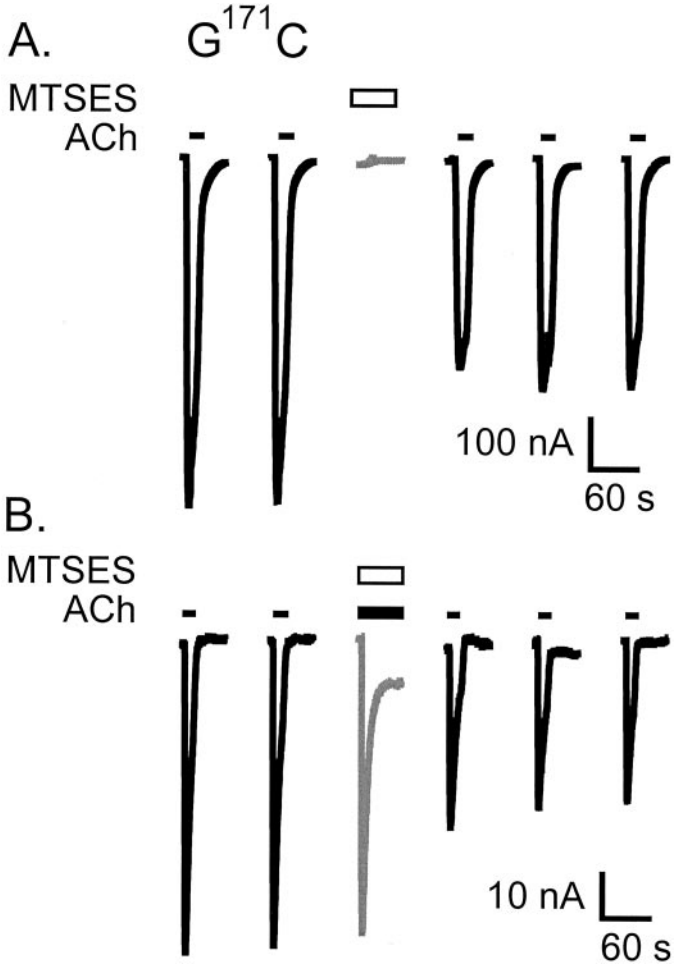

Fig. 8. MTSES modification of $G^{171}C$ is unchanged by ACh. A, 1 mM MTSES inhibited 22 ± 5% (n = 4) of ACh-evoked currents. B, MTSES plus 30 μM ACh inhibited 24 ± 5% (n = 4) of ACh-evoked currents. ▬, 10 μM ACh. The limiting dose for this mutant was 1 mM MTSES.

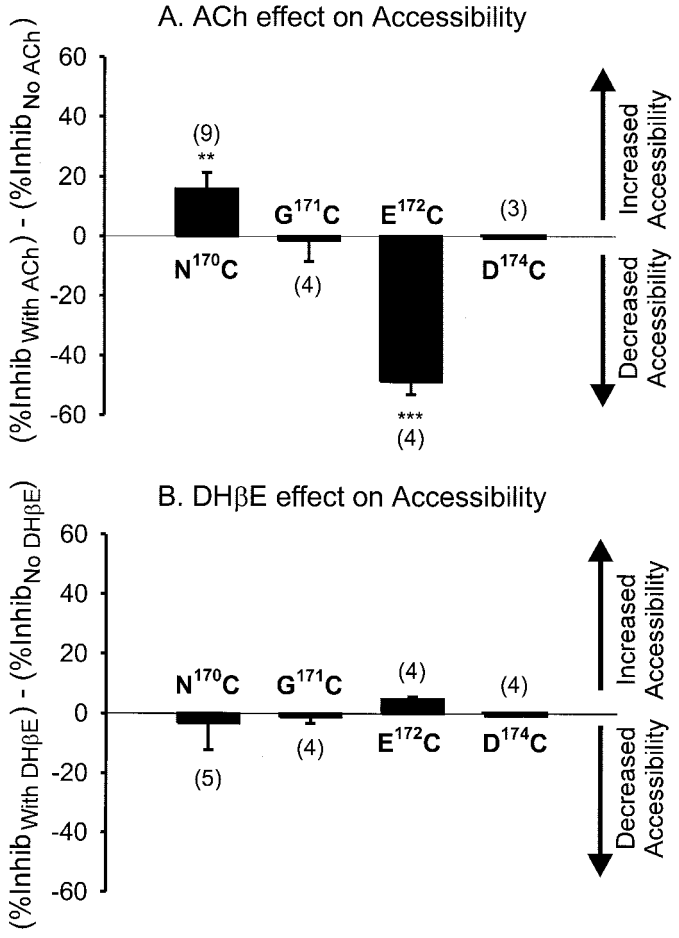

Fig. 9. Effects of ACh and DHβE on MTS modification. A, data are displayed as the percentage inhibition of ACh-evoked currents after MTS and ACh cotreatment minus that of MTS alone. MTSET data are shown for $N^{170}C$ and $E^{172}C$; MTSES data are shown for $G^{171}C$ and $D^{174}C$ because MTSET was a partial agonist of these receptors. (t test: ***, $p < 0.001$; **, $p < 0.005$). B, MTS ± DHβE. For all mutants except $E^{172}C$, data in B were recorded in ES-EGTA because DHβE was a partial agonist in ES-Ca^{2+}.

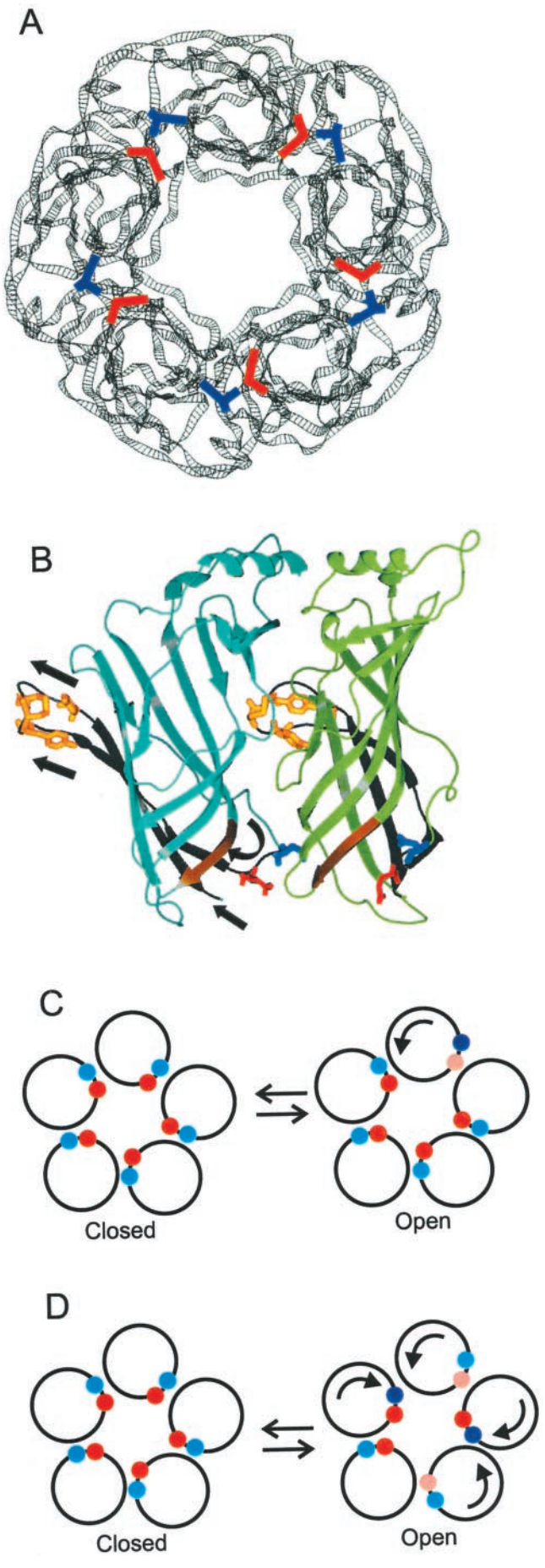

bition by MTSET increased to 30% (Fig. 7B). Thus, the effect of MTSET on $N^{170}C/L^{247}T$ $\alpha7$ receptors was greater in the presence than in the absence of ACh. The data suggest that $N^{170}C/L^{247}T$ $\alpha7$ receptors, unlike $E^{172}C/L^{247}T$ receptors, were modified to a greater extent in the activated state because of an increase in the accessibility of $N^{170}C$.

To determine whether the enhanced modification by MTSET of $N^{170}C/L^{247}T$ receptors depended on receptor activation, MTSET was coapplied with the antagonist DHβE. In ES-Ca^{2+}, DHβE was a partial agonist of $N^{170}C/L^{247}T$ $\alpha7$ receptors because the receptors retain the native E^{172} that is necessary for the Ca^{2+}-dependent activation of $L^{247}T$ receptors by antagonists (Eddins et al., 2002b). Thus, these experiments were carried out in ES-EGTA, in which DHβE was an antagonist with an IC_{50} of 2.6 μM (data not shown). In the absence of extracellular Ca^{2+}, DHβE evoked no responses from these receptors and had no effect on subsequent ACh-evoked currents (Fig. 7C). Modification by MTSET in the presence of DHβE caused an insignificant amount of inhibition (Fig. 7C). We infer that receptor activation, not simply occupancy of the ligand binding site, moves $N^{170}C$ into a more accessible position, whereas $E^{172}C$ moves to a less accessible position. These opposing effects are consistent with a shift in the position of loop 9 (see *Discussion*).

Reactivity of $G^{171}C$ to MTSET and MTSES Is the Same in the Presence and Absence of ACh. Like $E^{172}C/L^{247}T$ and $N^{170}C/L^{247}T$ $\alpha7$ receptors, modification of $G^{171}C/L^{247}T$ receptors by MTSET caused a partial inhibition (56 $\pm$ 3%, n = 4, data not shown). Unlike the other receptors, modification of $G^{171}C/L^{247}T$ $\alpha7$ receptors was the same in the presence of ACh (50 $\pm$ 4%, n = 3, data not shown). However, MTSET was a partial agonist of $G^{171}C/L^{247}T$ receptors, which could have confounded the results. Thus, MTSES, which was not an agonist of $G^{171}C/L^{247}T$ $\alpha7$ receptors, was used to assay the effects of agonist on modification. MTSES produced results similar to MTSET; the inhibition was the same in the presence and absence of ACh (Fig. 8). These data suggest that $G^{171}C$ is equally accessible to MTSES, regardless of receptor activation.

$D^{174}C/L^{247}T$ $\alpha7$ Receptors Are Not Inhibited by MTSET or MTSES. Treatment of $D^{174}C/L^{247}T$ $\alpha7$ nAChRs with 1 mM MTSET produced no effect on ACh-evoked currents when applied either in the presence (n = 4) or absence (n =

Fig. 10. Models of activation-induced conformational changes in the extracellular domain. A, homology model of the $\alpha7$ nAChR extracellular domain taken from the crystal structure of the AChBP (Brejc et al., 2001). This view is from the top of the receptor. The positions of N^{170} and E^{172} are shown in blue and red, respectively. Both residues are located in the intersubunit interface, but E^{172} is closer to the vestibule. B, two subunits of the $\alpha7$ homology model viewed from the lumen of the vestibule. N^{170} and E^{172} in loop 9 are shown in blue and red, respectively. A few of the residues in loop C that form the ligand binding site (Y^{187}, C^{189}, C^{190}, and Y^{194}) are shown in gold. The $\beta9$–$\beta10$ hairpin is shown in black, and the C-terminal end of $\beta1$ is brown. Arrows indicate the hypothetical intrasubunit movement of the $\beta9$–$\beta10$ hairpin and loop 9 during activation. C, diagram of symmetric rotation. Positions of N^{170} and E^{172} are indicated in blue and red, respectively. This model assumes that N^{170} is accessible from the outer surface, and E^{172} is accessible from the vestibule. In this model, one (or more) subunits rotate counterclockwise. N^{170} residues become more accessible, as indicated in dark blue. Upon activation, E^{172} becomes less accessible (pink) by moving deeper in the intersubunit interface. D, diagram of asymmetric rotation. In this model, accessibility of N^{170} and E^{172} is from the vestibule. N^{170} residues that would show an increase in accessibility in the open state are shown in dark blue. E^{172} positions that would show a decrease in accessibility are pink. The extent of rotation is exaggerated to illustrate the differences in accessibility from the vestibule. In this model, none of the residues is accessible from the outside surface.

4) of 30 μM ACh (data not shown). Similarly, MTSES (1 mM) also had no effect on $D^{174}C/L^{247}T$ receptors in the presence or absence of ACh ($n = 3$ each) (Fig. 9). Thus, $D^{174}C$ was either not accessible to MTSET or MTSES, or modification by these reagents had no functional effect.

Discussion

As summarized in Fig. 9A, ACh increased the modification of $N^{170}C$ and decreased the modification of $E^{172}C$ in $L^{247}T$ α7 nicotinic receptors. These effects were not observed in the presence of the antagonist DHβE (Fig. 9B), indicating that the effects of agonists required activation, not simply ligand binding. The ACh dose-dependence of inhibition of $E^{172}C$ modification was virtually identical with the dose-dependence of receptor activation by ACh. These data support the idea that receptor activation involves conformational changes near the N terminus of the β9 strand.

Model for Agonist-Driven Movements of Loop 9. Figure 10, A and B, shows a model of the α7 receptor from the AChBP crystal structure that we have used as a framework to interpret our results. The model shows that both E^{172} and N^{170} are in the intersubunit interface, but E^{172} is closer to and projects toward the vestibule, whereas N^{170} is buried more deeply (Fig. 10A). The model and previous results (Eddins et al., 2002b) suggest that $E^{172}C$ is accessible from the vestibule.

The question of how agonists can decrease the modification of $E^{172}C$ and increase the modification of $N^{170}C$ is also worth examining. Figure 10C shows a diagram in which activation causes the counterclockwise rotation of a single subunit. This model assumes that $N^{170}C$ becomes more accessible to MTSET from the outer surface, and $E^{172}C$ becomes less accessible to MTSET from the vestibule. This model could also apply to the rotation of several subunits. This model, however, is inconsistent with the ~15° clockwise rotation of α subunits proposed for *Torpedo californica* nAChRs (Unwin et al., 2002). To explain our results, clockwise rotations would require a ~60° rotational movement, which seems unlikely.

A second model in which pairs of adjacent subunits rotate asymmetrically during activation (Horenstein et al., 2001) is shown in Fig. 10D. This model assumes that MTS modifiers access both $E^{172}C$ and $N^{170}C$ from the vestibule. Clockwise rotation of one subunit of the pair would cause an increase in accessibility of $N^{170}C$ by moving it from a poorly accessible position in the intersubunit interface toward the vestibule. This clockwise rotation would not change the accessibility of $E^{172}C$ because it remains in a vestibule-lining position. The observed decrease in the accessibility of $E^{172}C$ is explained by the counterclockwise rotation of the other subunit of the pair, moving $E^{172}C$ away from the vestibule into the intersubunit interface. This counterclockwise rotation of this subunit would also shift $N^{170}C$ deeper into the interface, but because this residue was poorly accessible in the closed state, this decreased accessibility would be undetectable.

Our observations are also consistent with a model in which the activation of the receptor involves an intrasubunit movement (Fig. 10B). Ligand binding could transmit the activation signal via a shift in position of the β9–β10 hairpin structure, as suggested by Brejc et al. (2001). As shown in Fig. 10B, movement of the β9–β10 hairpin and loop 9 could increase the accessibility of $N^{170}C$ because of its movement from the intersubunit interface toward the vestibule. Simultaneously, the accessibility of $E^{172}C$ could be decreased by movement to a more protected position closer to the β1 strand. Alternatively, it is also possible that the movements of neighboring regions alter the accessibility of positions 170 and 172. Combinations of intrasubunit movement with either symmetric or asymmetric rotational movement of subunits could constitute part of the gating machinery. As described previously, conformational changes in the extracellular ligand binding domain could transmit activation signals to the "gate" in M2 via the β10–M1 linker and/or the M2–M3 linker (Grosman et al., 2000; Horenstein et al., 2001; Kash et al., 2003). Our results indicate that loop 9, in addition to loop 2 and the signature loop (loop 7) (Kash et al., 2003), undergoes agonist-driven conformational changes and may be an important part of the mechanism coupling ligand binding with the opening of the channel.

Acknowledgments

We thank Dr. Brenda Temple at the University of North Carolina at Chapel Hill R. L. Juliano Structural Bioinformatics Core Facility for assistance with molecular modeling.

References

Akabas MH, Stauffer DA, Xu M, and Karlin A (1992) Acetylcholine receptor channel structure probed in cysteine-substitution mutants. *Science (Wash DC)* **258:**307–310.

Bera AK, Chatav M, and Akabas MH (2002) $GABA_A$ receptor M2–M3 loop secondary structure and changes in accessibility during channel gating. *J Biol Chem* **277:** 43002–43010.

Brejc K, van Dijk WJ, Klaassen RV, Schuurmans M, van der Oost J, Smit AB, and Sixma TK (2001) Crystal structure of an ACh-binding protein reveals the ligand-binding domain of nicotinic receptors. *Nature (Lond)* **411:**269–276.

Eddins D, Lyford LK, Lee JW, Desai SA, and Rosenberg RL (2002a) Permeant but not impermeant divalent cations enhance activation of nondesensitizing α7 nicotinic receptors. *Am J Physiol* **282:**C796–C804.

Eddins D, Sproul AD, Lyford LK, McLaughlin JT, and Rosenberg RL (2002b) Glutamate 172, essential for modulation of $L^{247}T$ α7 ACh receptors by Ca^{2+}, lines the extracellular vestibule. *Am J Physiol* **283:**C1454–C1460.

Elgoyhen AB, Johnson DS, Boulter J, Vetter DE, and Heinemann S (1994) α9: an acetylcholine receptor with novel pharmacological properties expressed in rat cochlear hair cells. *Cell* **79:**705–715.

Elgoyhen AB, Vetter DE, Katz E, Rothlin CV, Heinemann SF, and Boulter J (2001) α10: a determinant of nicotinic cholinergic receptor function in mammalian vestibular and cochlear mechanosensory hair cells. *Proc Natl Acad Sci USA* **98:**3501–3506.

Galzi J-L, Bertrand S, Corringer P-J, Changeux J-P, and Bertrand D (1996) Identification of calcium binding sites that regulate potentiation of a neuronal nicotinic acetylcholine receptor. *EMBO (Eur Mol Biol Organ) J* **15:**5824–5832.

Gerzanich V, Peng X, Wang F, Wells G, Anand R, Fletcher S, and Lindstrom J (1995) Comparative pharmacology of epibatidine, a potent agonist for neuronal nicotinic acetylcholine receptors. *Mol Pharmacol* **48:**774–782.

Grosman C, Zhou M, and Auerbach A (2000) Mapping the conformational wave of acetylcholine receptor channel gating. *Nature (Lond)* **403:**773–776.

Hille B (2001) *Ion Channels of Excitable Membranes.* Sinauer Associates, Inc., Sunderland, MA.

Holden JH and Czajkowski C (2002) Different residues in the $GABA_A$ receptor α1T60-α1K70 region mediate GABA and SR-95531 actions. *J Biol Chem* **277:** 18785–18792.

Horenstein J, Wagner DA, Czajkowski C, and Akabas MH (2001) Protein mobility and GABA-induced conformational changes in $GABA_A$ receptor pore-lining M2 segment. *Nat Neurosci* **4:**477–485.

Jones S, Sudweeks S, and Yakel J (1999) Nicotinic receptors in the brain: correlating physiology with function. *Trends Neurosci* **22:**555–561.

Karlin A (2002) Emerging structure of the nicotinic acetylcholine receptors. *Nat Rev Neurosci* **3:**102–114.

Karlin A and Akabas MH (1995) Toward a structural basis for the function of nicotinic acetylcholine receptors and their cousins. *Neuron* **15:**1231–1244.

Karlin A and Akabas MH (1998) Substituted-cysteine accessibility method. *Methods Enzymol* **293:**123–145.

Kash TL, Jenkins A, Kelley JC, Trudell JR, and Harrison NL (2003) Coupling of agonist binding to channel gating in the $GABA_A$ receptor. *Nature (Lond)* **421:**272–275.

Le Novere N and Changeux J-P (1995) Molecular evolution of the nicotinic acetylcholine receptor: an example of multigene family in excitable cells. *J Mol Evol* **40:**155–172.

Lyford LK, Lee JW, and Rosenberg RL (2002) Low-affinity Ca^{2+} and Ba^{2+} binding sites in the pore of α7 nicotinic acetylcholine receptors. *Biochim Biophys Acta* **1559:**69–78.

McLaughlin JT, Hawrot E, and Yellen G (1995) Covalent modification of engineered cysteines in the nicotinic acetylcholine receptor agonist-binding domain inhibits receptor activation. *Biochem J* **310:**765–769.
Panicker S, Cruz H, Arrabit C, and Slesinger PA (2002) Evidence for a centrally located gate in the pore of a serotonin-gated ion channel. *J Neurosci* **22:**1629–1639.
Revah F, Bertrand D, Galzi J-L, Devillers-Thiéry A, Mulle C, Hussy N, Bertrand S, Ballivet M, and Changeux J-P (1991) Mutations in the channel domain alter desensitization of a neuronal nicotinic receptor. *Nature (Lond)* **353:**846–849.
Role LW and Berg DK (1996) Nicotinic receptors in the development and modulation of CNS synapses. *Neuron* **16:**1077–1085.
Sine SM and Steinbach JH (1984) Agonists block currents through acetylcholine receptor channels. *Biophys J* **46:**277–283.
Teissere JA and Czajkowski C (2001) A β-strand in the γ2 subunit lines the benzodiazepine binding site of the $GABA_A$ receptor: structural rearrangements detected during channel gating. *J Neurosci* **21:**4977–4986.
Unwin N, Miyazawa A, Li J, and Fujiyoshi Y (2002) Activation of the nicotinic acetylcholine receptor involves a switch in conformation of the α subunits. *J Mol Biol* **319:**1165–1176.
Wilson G and Karlin A (2001) Acetylcholine receptor channel structure in the resting, open and desensitized states probed with the substituted-cysteine-accessibility method. *Proc Natl Acad Sci USA* **98:**1241–1248.

Address correspondence to: Dr. Robert L. Rosenberg, Department of Pharmacology, CB #7365, University of North Carolina at Chapel Hill, Chapel Hill, NC 27599-7365. E-mail: bobr@med.unc.edu